



The 1<sup>st</sup> Mediterranean Conference on Fracture and Structural Integrity, MedFract1

## Effect of manufacturing parameters on tensile properties of FDM printed specimens

Cristina Vălean<sup>a</sup>, Liviu Marșavina<sup>a,\*</sup>, Mihai Mărghițaș<sup>a</sup>, Emanoil Linul<sup>a</sup>,  
Javad Razavi<sup>b</sup>, Filippo Berto<sup>b</sup>

<sup>a</sup>*Department of Mechanics and Strength of Materials, Politehnica University of Timisoara,  
1 Mihai Viteazu Avenue, Timisoara 300 222, Romania*

<sup>b</sup>*Department of Mechanical and Industrial Engineering, Norwegian University of Science and Technology (NTNU),  
Richard Birkelands vei 2b, 7491, Trondheim, Norway*

---

### Abstract

Nowadays, one of the most studied technologies for obtaining different parts is Additive Manufacturing (AM). Whether it is about plastic or metal materials, AM is used because very complex parts can be obtained, without further technological operations. From all AM technologies, Fused Deposition Modeling (FDM) is the most used all over the world, due to its cost-effective way of printing. FDM is based on the extrusion of a wire, through which a piece is formed by successively depositing layer-by-layer of molten material. This paper experimentally investigates the tensile properties of 3D printed specimens obtained through FDM printing. The influence of spatial printing direction (0°, 45°, 90°) and size effect (different thickness) on main mechanical properties was investigated. Polylactic acid (PLA) dog bone specimens were adopted for all tensile tests. Experimental tests were carried out at room temperature, according to ISO 527-1 Standard. It was observed that the spatial orientation has less influence on the Young modulus and higher influence on the tensile strength. Furthermore, increasing the number of layers leads to decreasing of both the Young modulus and tensile strength.

© 2020 The Authors. Published by Elsevier B.V.

This is an open access article under the CC BY-NC-ND license (<http://creativecommons.org/licenses/by-nc-nd/4.0/>)

Peer-review under responsibility of MedFract1 organizers

*Keywords:* Additive Manufacturing; FDM; printing directions; tensile properties.

---

---

\* Corresponding author. Tel.: +40-256-403577.; fax: +40-256-403523.

E-mail address: [liviu.marsavina@upt.ro](mailto:liviu.marsavina@upt.ro)

## 1. Introduction

Additive manufacturing (AM) is a growing technology enabling the production of complex objects. The AM technology is able to print almost any material (e.g. metals and their alloys, ceramics, polymers, biological materials, etc.), offering a wide range of products in different range of engineering applications, such as the automotive, aerospace, civil, medical, energy, sport industries (García Plaza et al. (2019); Stoia et al. (2019a)).

Liquid-based and powder-based processes are used to produce polymers and polymer-like AM materials. Polymers used in AM processes are typically thermoplastic filaments, resins or powders. From all AM technologies, Fused Deposition Modeling (FDM) is the most used all over the world, due to its cost-effective way of printing and the ease of obtaining parts. In FDM process, the 3D printing machine contains a plastic wire spool (e.g. polycarbonate - PC, acrylonitrile butadiene styrene - ABS, polyphenylsulfone - PPSF, polyethyleneterephthalate - PET, polylactic acid - PLA, polyamide - PA, PC-ABS blends, etc.) feeding a print head (nozzle) which extrudes thin filament of melted plastic, forming, layer-by-layer, the component according to a CAD file (Masood (1996); Mohamed et al. (2015)).

### Nomenclature

ABS	acrylonitrile butadiene styrene
AM	additive manufacturing
DB	dog-bone specimens
E	Young's Modulus
FDM	fused deposition modeling
PA	polyamide
PC	polycarbonate
PET	polyethyleneterephthalate
PLA	polylactic acid
PO	printing orientations
PPSF	polyphenylsulfone
t	thickness of the samples
W	width of the samples
$\sigma_m$	tensile strength

Many papers in the literature evaluate the mechanical behavior of materials using AM technologies (Feng et al. (2019); Wang et al. (2019)). However, limited studies are focused on the FDM process. Process main parameters that strongly affect the properties of AM 3D printed parts are layer thickness, raster orientation, building orientation and nozzle temperature (Linul et al. (2020); Stoia et al. (2020)). Es-Said et al. (2000) investigated the effect of layer orientation on mechanical properties (tensile strength, modulus of rupture and impact resistance) of rapid prototyped specimens. The authors found that the 0° orientation, where layers were deposited along the length of the specimens, highlighted superior properties, while the lowest ones were obtained for 45° orientation. They observed that the fracture paths of all the specimens always occurred along the layer interface. Maloch et al. (2018) studied the influence of the extrusion nozzle and the layer thickness on the mechanical properties (tensile and flexural strength, tensile and flexural modulus) of the ABS printed specimens. The authors observed that the best properties are obtained for small thicknesses of the layers. They also noted that an increase of the nozzle temperature ensures better melting between adjacent layers. Rodríguez-Panes et al. (2018) present a comparative study of the tensile behavior (tensile yield stress, tensile strength, nominal strain at break and modulus of elasticity) of different parts produced by FDM technique, using PLA and ABS thermoplastic materials. The test specimens manufactured using PLA are stiffer and have a tensile strength higher than ABS. On the other hand, the results obtained with ABS exhibit a lower variability than those obtained with PLA. Tensile characterization of ABS and PC parts was performed by Cantrell et al. (2017) to determine the extent of anisotropy present in 3D printed materials. Their ABS results indicated that build and raster orientation had a slight effect on the Young's modulus and Poisson's ratio. Raster orientation of PC specimens reveal anisotropic behavior, the moduli and strengths varied by up to 20%. Warnung et al. (2018) mechanically characterized, using

FDM process, 8 types of materials. They observed that 3D printing with PA wire generated the strongest material, while the stiffest material was produced by using a wire made of PET reinforced with carbon fibers.

This paper experimentally investigates the tensile properties of PLA printed specimens obtained through FDM technology. Considering that there are still some ambiguities related to the influence of certain process parameters, the influence of building orientation ( $0^\circ$ ,  $45^\circ$ ,  $90^\circ$ ) and size effect (different thickness) on main tensile properties were evaluated. Furthermore, the relative errors for thickness and width of the 3D printed specimens have been investigated from dimensional perspective.

## 2. Materials and manufacturing process

Polylactic acid (PLA) is a bio-based and bio compostable thermoplastic that is widely used in different industries for due to its superior mechanical strength. Unlike the high strength and high stiffness of this material, its brittle behavior and low heat distortion temperature have been pointed out to be its limitations in real life, Sennan et al. (2014). Due to the mentioned characteristics of PLA, it has been widely considered as a model material in FDM printing. The FDM parts produced by PLA filaments tend to provide mechanical properties comparable to the ones made from bulk PLA Farah et al. (2016), Yao et al. (2020), Zhao et al. (2019). WN400 3D platform printer was used for fabrication of the test specimens. The printer was equipped with an HFE300 extruder for printing parts with filaments of 2.85 mm diameter. 3D printing software was used to set the printing parameters such as raster angle, head speed, temperature and so on. To ensure the quality of the printed part, the temperature of the nozzle and the built platform was controlled at around  $60^\circ\text{C}$  and  $220^\circ\text{C}$ , respectively. Was defined an infill density of 100% in the printing software with raster angles of  $\pm 45$  degrees for the infill and different layer thicknesses were considered to print layers.

Following the 3D printing process, dog-bone (DB) specimens were obtained. The geometrical parameters of the DB specimens followed the ISO 527-1 (2012) standard recommendations (Fig. 1a).

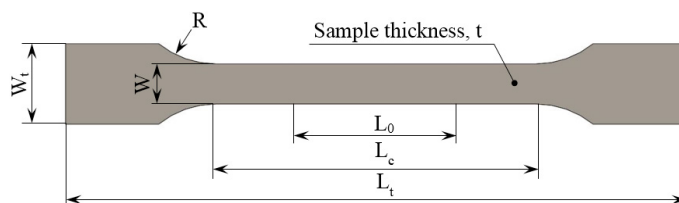


Fig. 1. Geometrical parameters of the DB specimens

In order to obtain the main geometrical and tensile properties of the FDM printed specimens, different printing orientations (PO) were used. Figure 2 shows a schematic view of the PO ( $0$ ,  $45$  and  $90^\circ$ ). In the same figure, the growing direction is presented; therefore, all specimens were manufactured in a horizontal plane.

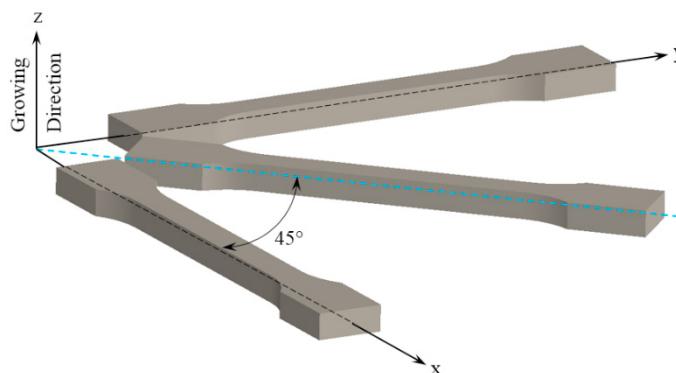


Fig. 2. Printing orientation of 3D specimens

Furthermore, in order to highlight the size effect, some of the specimens were printed with different thicknesses (see Table 1). For simplicity, the following naming convention is adopted in this text: specimen (DB) – specimen thickness (1.25, 2.15, 3.70, 4.00 or 8.00) – printing orientation (0, 45 or 90). As an example, DB-2.15-0 corresponds to a DB specimen with a thickness of 2.15 mm obtained at a PO of 0°.

Table 1. Specimen's description

Effect of	Specimen code	Thickness [mm]	Width [mm]	Orientation angle [°]
Thickness	DB-1.25-0	1.25	6	0
	DB-2.15-0	2.15	7	0
	DB-3.70-0	3.70	13	0
	DB-8.00-0	8.00	13	0
Printing orientation	DB-4.00-0	4.00	10	0
	DB-4.00-45	4.00	10	45
	DB-4.00-90	4.00	10	90

### 3. Tensile tests

Tensile tests were performed on a 5 kN Zwick Roell 005 electromechanical testing machine, according to ISO 527-1 (2012) standard. All tests run up to the failure point with a loading speed of 2 mm/min, at room temperature. A clip-on extensometer, with calibrated distance 30 mm was used for measuring strains, instead of the crosshead displacement of testing machine. For each type of specimen were tested a number of five specimens. Figure 3 shows the DB specimen in the tensile testing machine grips together with the positioning of the extensometer, both before (Fig. 3a) and after (Fig. 3b) the experimental test.

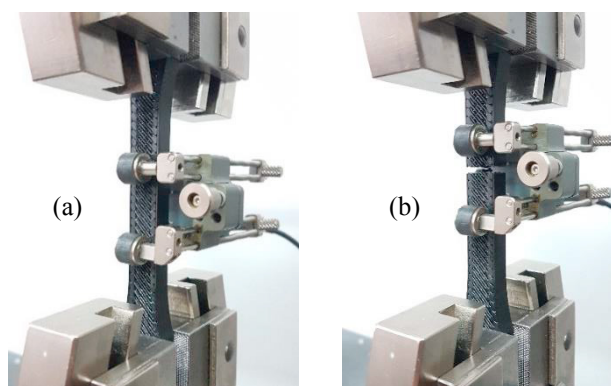


Fig. 3. Tensile specimen before (a) and after (b) tensile test

### 4. Results and discussions

Relative thickness and width of the DB specimens have been investigated from dimensional perspective. The geometrical errors were calculated as the ratio between the real (measured) and the nominal (designed) size. Theoretical dimensions and real measurements of the specimen's size were used in computation of geometric errors of width and thickness in Z-axis (Stoia et al. (2019b); Rajak et al. (2019)). Each measurement was performed 3 times, and the average value of the dimensions, at each PO, was used for plotting. Figure 4 shows the variation of the relative errors according to the PO. Regardless of PO, both geometric parameters (thickness and width) have relative errors below 4%, which means a good dimensional accuracy. However, the width errors are approximately double that of the thickness errors. This aspect can be associated with the different size of the specimens on the two directions, the

width being 3 times larger than the thickness. Regarding the orientation effect, both dimensions exhibit almost the same tendency with increasing of PO. Thickness errors have a maximum easily detectable at  $45^\circ$ , and those of width vary linearly with PO, in the range  $0$ - $90^\circ$ . On the other hand, the smallest  $t$  errors are obtained for a PO of  $90^\circ$  (1.52%), while  $W$  experiences the most favorable errors for the PO of  $0^\circ$  (2.5%).

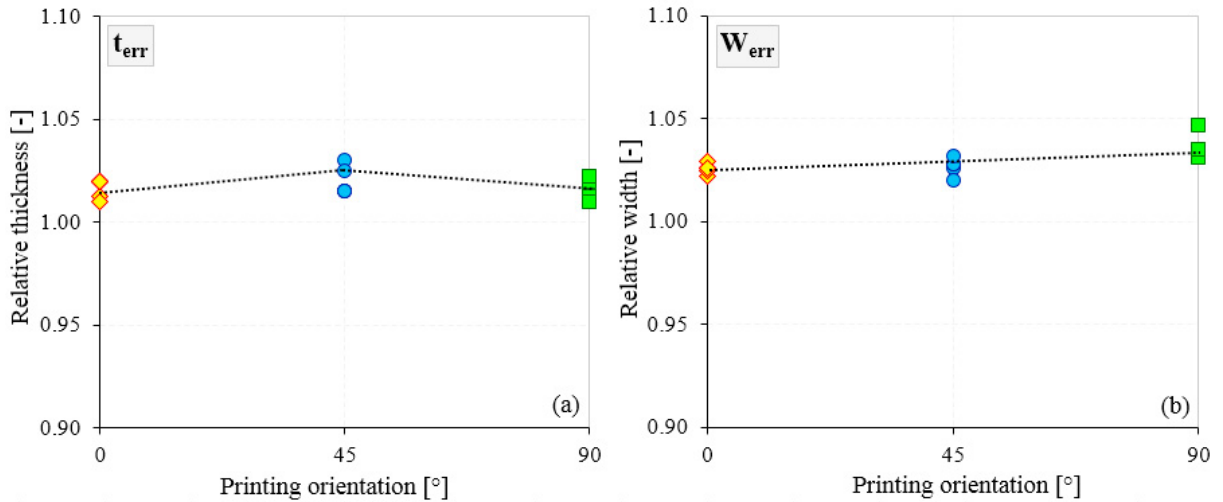


Fig. 4. Geometric errors of thickness (a) and width (b) according to PO

After the tensile tests, the load and displacement data, for each group of specimens, were obtained and processed (Aliha et al. (2019); Marsavina et al. (2010); Voiconi et al. (2014)). Figure 5 shows the load-displacement curves of DB specimens according to the PO. All curves show a linear elastic zone from which the Young's modulus is determined according to ISO 527-1 (2012) standard. Beyond this zone, the curves have a maximum point easily identifiable. This maximum load is used to determine the tensile strength of the DB specimens. It can be easily observed that the DB-4.00-0 and DB-4.00-90 specimens have approximately the same fracture load ( $\sim 2100$  N). Moreover, both the fracture loads ( $\sim 1950$  N) and the displacements corresponding to them ( $\sim 7$  mm) almost coincide for the two PO. On the other hand, compared with the PO of  $0^\circ$  and  $90^\circ$ , the  $45^\circ$  one presents lower values for all the maximum load ( $\sim 1980$  N), the fracture load ( $\sim 1800$  N) and the displacement at the fracture load ( $\sim 4.5$  mm).

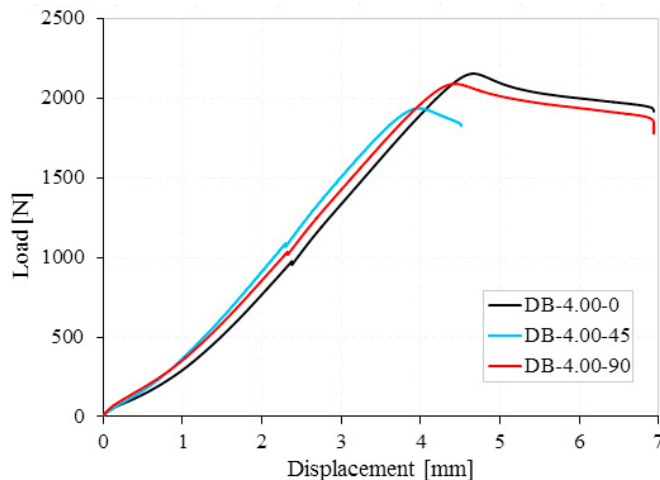


Fig. 5. Load-displacement curves for DB-4.00-0/45/90 specimens

Figure 6 shows variation of the Young’s Modulus and the tensile strength with the PO. As mentioned above, due to the almost overlap of the linear-elastic zones, the specimens have almost the same value of the Young’s Modulus. Insignificantly higher values, of only 1.18%, can be observed in the case of DB-4.00-90 specimens, compared to the DB-4.00-45 ones. Moreover, this variation of the properties can be associated with a linear trendline. An aspect to note is that for the DB-4.00-90 specimen, the highest standard deviations of the results are obtained (~ 216 MPa), while at the opposite pole is DB-4.00-45 specimen (~ 31 MPa). On the other hand, the tensile strength shows significant differences with the change of the PO. In this case, it can be seen that the highest values are found for the DB-4.00-0 specimens (50.88 MPa), while the lowest values (46.77 MPa) are presented by the DB-4.00-45 specimens. All the results, regardless of the PO, present errors below 1.5%.

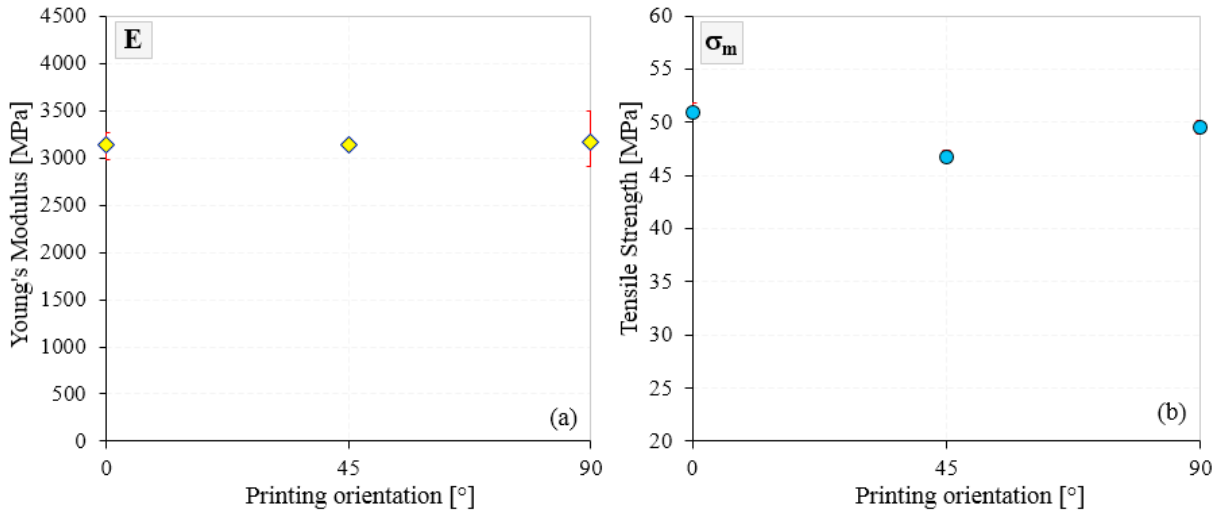


Fig. 6. Influence of PO on Young’s Modulus (a) and tensile strength (b) properties

In the last part of the paper, we investigated the influence of the size effect on the main mechanical properties of the 3D printed specimens. Figure 7 shows the variation of Young’s Modulus and tensile strength with the thickness of the tested specimens.

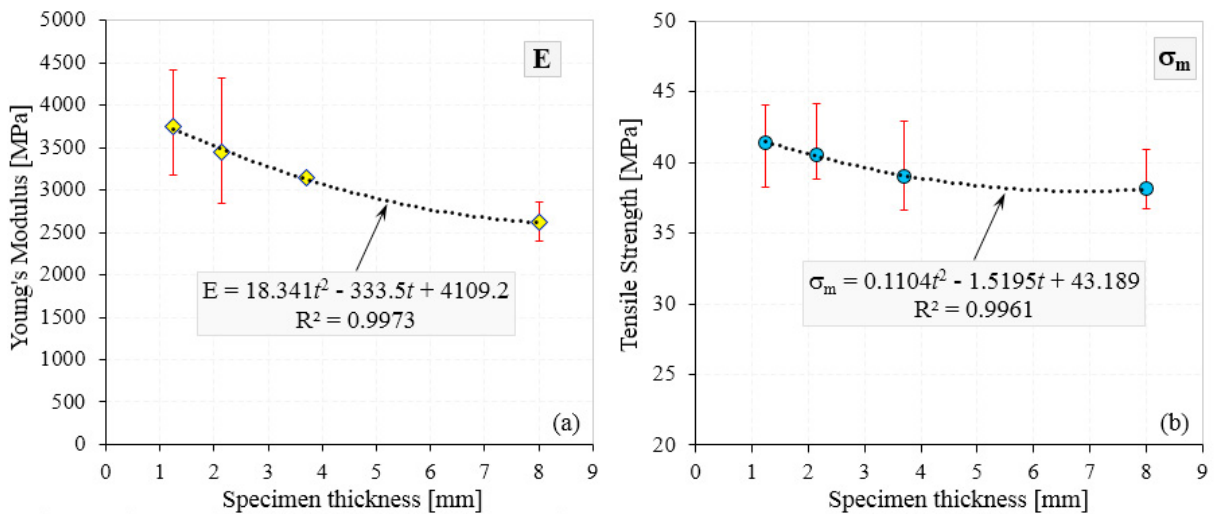


Fig. 7. Influence of specimen thickness on Young’s Modulus (a) and tensile strength (b) properties

The two properties ( $E$  and  $\sigma_m$ ) have the same pattern and will be discussed together. So that the results can be compared, all the DB specimens were manufactured using the same PO, namely  $0^\circ$ . It is observed that the best properties are obtained in case of DB-1.25-0 specimen, the properties decreasing polynomial with increasing the thickness of the specimens, from 1.25 to 8 mm (DB-8.00-0). Therefore, between the extreme thicknesses of the specimens a difference of over 30% for  $E$  and over 7% for  $\sigma_m$  is obtained. It seems that as the size of the specimen's increases, the number of defects increases, which leads to a fracture of the specimens to smaller loading forces. Except for DB-3.70-0 specimen, all the other specimens show significant standard deviations of the results. However, the regression laws have the coefficient of determination ( $R^2$ ) of over 0.996, which means a good matching of the results. The two obtained polynomial laws help to obtain the Young's Modulus and tensile strength, in the range of 1.25-8 mm thicknesses, without carrying out supplementary experimental tensile tests.

## 5. Conclusions

This paper investigates the tensile behavior of 3D printed specimens. Among the Additive Manufacturing (AM) technologies, the Fused Deposition Modeling (FDM) process was considered, while Polylactic acid (PLA) was used as the filament material. The experimental tests were performed on standardized dog-bone specimens and the main process parameters (printing orientation-PO and layer thickness/size effect) were analyzed.

The following conclusions can be drawn:

- The main geometric parameters (thickness- $t$  and width- $W$ ) of the specimens have relative errors below 4%; however, the  $W$  errors are approximately double that of the  $t$  ones.
- The Young's Modulus ( $E$ ) changes by only 1.8% depending on the PO, while tensile strength ( $\sigma_m$ ) shows differences of over 8%, between the extreme values. Regardless of the PO,  $E$  and  $\sigma_m$  have errors below 1.5%.
- Both  $E$  and  $\sigma_m$  decrease significantly and polynomial with increasing sample sizes (30% for  $E$  and over 7% for  $\sigma_m$ ). Therefore, due to the presence of the inherent defects, a strong size effect is identified, especially for  $E$ .
- The determined values of tensile strength for PLA obtained through AM are in good agreement with those from injection molded (yellow region in Fig. 8), except of  $45^\circ$  orientation which are a little bit lower.

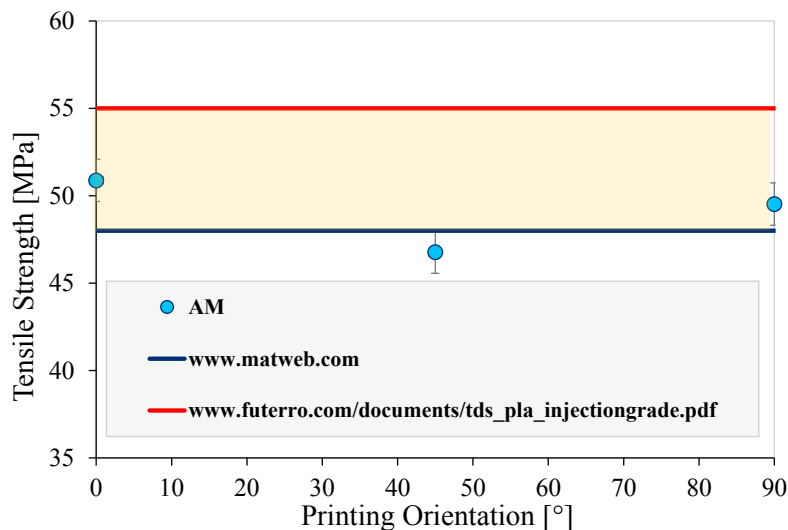


Fig. 8. A comparison between tensile strength of PLA obtained by AM and injection molded

## Acknowledgements

The project leading to these results has received funding from the European Union's Horizon 2020 research and innovation program under grant agreement No. 857124.

## References

- Aliha, M.R.M., Mousavi, S.S., Bahmani, A. et al., 2019. Crack initiation angles and propagation paths in polyurethane foams under mixed modes I/II and I/III loading, *Theoretical and Applied Fracture Mechanics*, 101, 152-161.
- Cantrell, J., Rohde, S., Damiani, D., 2017. Experimental Characterization of the Mechanical Properties of 3D-Printed ABS and Polycarbonate Parts. *Rapid Prototyping Journal*, 23(4), 811-824.
- Es-Said, O.S., Foyos, J., Noorani, R., et al., 2000. Effect of layer orientation on mechanical properties of rapid prototyped samples. *Materials and Manufacturing Processes*, 15(1), 107-122.
- Farah, S., Anderson, D.G., Langer, R., 2016. Physical and mechanical properties of PLA, and their functions in widespread applications – a comparative review. *Advanced Drug Delivery Reviews* 107, 367-392.
- Feng, L., Wang, Y., Wei, Q., 2019. PA12 powder recycled from SLS for FDM. *Polymers*, 11, 727.
- García Plaza, E., López, P.J.N., Torija, M.Á.C., Muñoz, J.M.C., 2019. Analysis of PLA geometric properties processed by FFF additive manufacturing: Effects of process parameters and plate-extruder precision motion. *Polymers*, 11, 1581.
- ISO 527-1, 2012. *Plastics-Determination of Tensile Properties-part 1: General Principles*. International Organization for Standardization; ISO: Geneva, Switzerland, 23.
- Linul, E., Marsavina, L., Stoia, D.I., 2020. Mode I and II fracture toughness investigation of Laser-Sintered Polyamide. *Theoretical and Applied Fracture Mechanics*, 106, 102497.
- Maloch, J., Hnátková, E., Žaludek, M., Krátký, P., 2018. Effect of processing parameters on mechanical properties of 3D printed samples. In *Materials Science Forum* (Vol. 919, pp. 230-235). Trans Tech Publications.
- Marsavina, L., Cernescu, A., Linul, E. et al., 2010. Experimental determination and comparison of some mechanical properties of commercial polymers. *Materiale Plastice*, 47, 85-89.
- Masood, S. H., 1996. Intelligent rapid prototyping with fused deposition modelling. *Rapid Prototyping Journal*, 2(1), 24-33.
- Mohamed, O.A., Masood, S. H., Bhowmik, J. L., 2015. Optimization of fused deposition modeling process parameters: a review of current research and future prospects. *Advances in Manufacturing*, 3(1), 42-53.
- Rajak, D.K., Pagar, D.D., Menezes, P.L., et al., 2019. Fiber reinforced polymer composites: Manufacturing, properties, and applications. *Polymers*, 11, 1667.
- Rodríguez-Panes, A., Claver, J., Camacho, A.M., 2018. The influence of manufacturing parameters on the mechanical behaviour of PLA and ABS pieces manufactured by FDM: A comparative analysis. *Materials*, 11, 1333
- Sennan, P., Pumchusak, J., 2014. Improvement of mechanical properties of poly(lactic acid) by elastomer. *The Malaysian Journal of Analytical Sciences* 18(3) 669-675.
- Stoia, D.I., Linul, E., Marşavina, L., 2019a. Influence of manufacturing parameters on mechanical properties of porous materials by Selective Laser Sintering. *Materials*, 12, 871.
- Stoia, D.I., Marşavina, L., Linul, E., 2019b, Correlations between process parameters and outcome properties of Laser-Sintered Polyamide. *Polymers*, 11, 1850.
- Stoia, D.I., Marsavina, L., Linul, E., 2020. Mode I Fracture Toughness of Polyamide and Alumide Samples obtained by Selective Laser Sintering Additive Process. *Polymers*, 12, 640.
- Voiconi, T., Linul, E., Marsavina, L. et al., 2014. Determination of flexural properties of rigid PUR foams using digital image correlation, *Solid State Phenomena*, 216, 116-121.
- Wang, X., Zhao, L., Fuh, J.Y.H., Lee, H.P., 2019. Effect of porosity on mechanical properties of 3D printed polymers: Experiments and micromechanical modeling based on X-ray computed tomography analysis. *Polymers*, 11, 1154.
- Warnung, L., Estermann, S., Reisinger, A., 2018. Mechanical properties of Fused Deposition Modeling (FDM) 3D printing materials. *RTEjournal - Fachforum für Rapid Technologien*, Vol. 2018.
- Yao, T., Ye, J., Deng, Z., et al., 2020. Tensile failure strength and separation angle of FDM 3D printing PLA material: Experimental and theoretical analyses. *Composites Part B* 188, 107894.
- Zhao, Y., Chen, Y., Zhou, Y., 2019. Novel mechanical models of tensile strength and elastic property of FDM AM PLA materials: Experimental and theoretical analyses. *Materials and Design* 181, 108089.
- \*\*\* <http://www.matweb.com/>
- \*\*\* [http://www.futero.com/documents/tds\\_pla\\_injectiongrade.pdf](http://www.futero.com/documents/tds_pla_injectiongrade.pdf)